

MLCT Excited-State Properties of the Ru(L)₂(CN)₂ (L = 2-(N-Methylformimidoyl)pyridine) Complex. A Theoretical Approach by Means of DV–X α Molecular Orbital Calculations

Mutsuhiro Maruyama, Hideyo Matsuzawa,[†] and Youkoh Kaizu*

Department of Chemistry, Tokyo Institute of Technology, O-okayama, Meguro-ku, Tokyo, Japan

Received June 3, 1994[⊗]

A new luminescent compound of Ru(imin)₂(CN)₂, where imin is 2-(N-methylformimidoyl)pyridine, which has smaller π electron system than bpy and phen is synthesized. The ¹MLCT absorption maximum of this complex is nearly identical with that of Ru(bpy)₂(CN)₂ and Ru(phen)₂(CN)₂, while the emission from the ³MLCT state of the former is highly red-shifted in comparison with that of the latter. The Stokes shift (ΔE_{ST}), which is the energy difference between the ¹MLCT absorption maximum and the emission maximum, of Ru(imin)₂(CN)₂ in protic and aprotic solvents shows the good correlation with the solvent acceptor number (AN) and the solvent dielectric parameter, respectively, similar to those of Ru(bpy)₂(CN)₂ and Ru(phen)₂(CN)₂. However, the solvent dependence of ΔE_{ST} of the former is weak compared with that of the latter both in protic and aprotic solvents. DV–X α calculations show that (i) the electronic density on CN is less decreased for Ru(imin)₂(CN)₂ in the MLCT excited states compared with that for the L = bpy and phen analogues and that (ii) the decrease of the dipole moment of Ru(imin)₂(CN)₂ in the excited state is smaller than that of the others. The weak solvent dependence of ΔE_{ST} for Ru(imin)₂(CN)₂ in protic solvents is considered to come from the small decrease of the electronic density on CN, which makes the solvent reorganization caused from the change of the Lewis acidity of CN smaller. The weak solvent dependence of Ru(imin)₂(CN)₂ in aprotic media is accounted for by the small dielectric reorganization of the solvents in the excited state due to the small decrease of the dipole moment of this molecule. The large ΔE_{ST} of Ru(imin)₂(CN)₂ comes from the inner-sphere reorganization of the less rigid C=N bond of the methylimine on which the promoted electron is relatively localized in the lowest MLCT states.

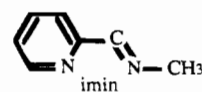
Introduction

Electronic redistribution caused by light excitation often provides the molecule in the excited state with new properties which are absent in the ground state. The Dicyanobis-(polypyridine)ruthenium(II) complex, abbreviated as Ru(L)₂(CN)₂, is known to show the strong solvatochromic MLCT absorption and emission.^{1,2} Since the solvatochromism correlates with the solvent acceptor number (AN), the specific acid–base interaction between the CN and the solvent is considered to be the reason for such phenomena. Interestingly, the solvent dependence of the emission maxima of Ru(L)₂(CN)₂ is weak compared with that of the absorption maxima,¹ which is attributed to the decrease of the electronic density on CN in the excited state.^{1,2} The decrease of the charge on CN is also suggested by the early work of Peterson and Demas,³ who had found that the proton attached on the CN in the aqueous acid is released by light excitation. In addition to such an interesting excited-state property, the coordinating ability to other ions at

the CN unit of this complex has made it the subject of much attention recently for designing the supramolecular redox systems.^{4,5a}

In spite of the extensive work concerning Ru(L)₂(CN)₂,^{1–6} however, it has not clarified how the electronic density on CN decreases in the MLCT transition. Although such a transition should accompany the change of the dipole moment of the molecule, which will determine the extent of the dielectric solvent reorganization in the excited state, the qualitative and the quantitative investigation for it have not been performed yet. To understand the electronic flow of this complex in the excited state, we conducted DV–X α molecular orbital calculations on Ru(L)₂(CN)₂ in this paper, which enabled us to estimate the change of the electronic density on three units (i.e., Ru, L, and CN) in the MLCT excited states. Using the calculated net charge on each atom in the ground and the excited states, we could also estimate the change of the dipole moment caused from the electronic redistribution in the excited states.

As for the MLCT excited-state of Ru(L)₂(CN)₂, there remain the following questions about the relationship between the size of the π electron systems of L and the electronic flow in the excited state: (i) To what extent does the size of the π electron system of L affect the charge redistribution of Ru(L)₂(CN)₂ in the excited state? (ii) How does it affect the decrease of the electronic density on CN and the change of the dipole moment in the excited state? To clarify these points, we synthesized a new luminescent complex Ru(imin)₂(CN)₂, where imin = 2-(N-



methylformimidoyl)pyridine, which has smaller π electron system than L = bpy or phen, and compared the excited-state

* To whom correspondence should be addressed.

[†] Department of Chemistry, School of Science, Kitasato University, Kitasato, Sagami-hara, Kanagawa, Japan.

[⊗] Abstract published in *Advance ACS Abstracts*, May 15, 1995.

- (1) (a) Belser, P.; von Zelewsky, A.; Juris, A.; Barigelletti, F.; Balzani, V. *Gazz. Chim. Ital.* **1985**, *115*, 723. (b) Juris, A.; Barigelletti, F.; Balzani, V.; Belser, P.; von Zelewsky, A. *J. Chem. Soc., Faraday Trans. 2* **1987**, *83*, 2295.
- (2) Kitamura, N.; Sato, M.; Kim, H.-B.; Obata, R.; Tazuke, S. *Inorg. Chem.* **1988**, *27*, 651.
- (3) (a) Peterson, S. H.; Demas, J. N. *J. Am. Chem. Soc.* **1976**, *98*, 7880. (b) Peterson, S. H.; Demas, J. N. *J. Am. Chem. Soc.* **1979**, *101*, 6571.
- (4) (a) Bignozzi, C. A.; Argazzi, R.; Schoonover, J. R.; Gordon, K. C.; Dyer, R. B.; Scandola, F. *Inorg. Chem.* **1992**, *31*, 5260. (b) Amadelli, R.; Argazzi, R.; Bignozzi, C. A.; Scandola, F. *J. Am. Chem. Soc.* **1990**, *112*, 7099. (c) Bignozzi, C. A.; Argazzi, R.; Garcia, C. G.; Scandola, F. *J. Am. Chem. Soc.* **1992**, *114*, 8727.

properties of this complex with those of Ru(bpy)₂(CN)₂ and Ru(phen)₂(CN)₂. We found out that both the decrease of the electronic density on CN and the change of the dipole moment of Ru(imin)₂(CN)₂ in the MLCT excited state are smaller than those of the L = bpy or phen analogues.

Experimental Section

Apparatus and Measurements. The absorption spectra were determined on the Hitachi Model 330 spectrophotometer. The emission spectra of Ru(bpy)₂(CN)₂ and Ru(phen)₂(CN)₂ were determined on a Hitachi 850 fluorescence spectrophotometer equipped with a Hamamatsu R928 photomultiplier. Emission spectra of Ru(imin)₂(CN)₂ were determined by means of a single-photon-counting method, which is more sensitive in the red. The sample was excited at 514.5 nm from an Ar-ion laser system, and the emission was detected through a monochromator (Nikon P-250) by a Hamamatsu photomultiplier R316 (S1 sensitivity) equipped with a photomultiplier cooler (HTV Model C659). The emission spectra were corrected with the standard solution of 4-dimethylamino-4'-nitrostilbene for both systems.⁷ The spectra determined by the Hitachi 850 for Ru(imin)₂(CN)₂ and Ru(bpy)₂(CN)₂ were identical with those by the single-photon-counting method.

The cyclic voltammetry was carried out on the same instrument mentioned previously.⁸ The measurement was performed against the Ag(s)/AgNO₃ (0.1 M) in CN₃CN reference electrode. All the spectroscopic and electrochemical measurements described above were carried out at room temperature, and the solvents used for these measurements were purified according to the literature.⁹

¹H-NMR spectra were measured in CD₃OD solutions on the JEOL-400EX FT-NMR system, and the signal of the methyl proton of CH₃OD was used as the internal standard (3.35 ppm). The lifetimes of Ru(L)₂(CN)₂ (L = bpy, phen) were measured using the Nd³⁺:YAG laser system described previously.⁸ The lifetimes of Ru(imin)₂(CN)₂ were measured by the single-photon-counting method on the PRA nanosecond fluorometer system. The sample was excited at 300–400 nm from a PRA 510B nitrogen gas lamp through a monochromator (Jobin-Yvon H-10). Emission whose wavelength was longer than 700 nm was detected through a glass filter by a Hamamatsu photomultiplier R928 and counted on a Norland Model 5300 multichannel analyzer. The double wall cell compartment was thermostated at 298 K by a Haake FK thermostat.

Materials. Ru(bpy)₂(CN)₂ and Ru(phen)₂(CN)₂ were prepared according to the literature¹⁰ and purified by column chromatography (Wako gel) with methanol. The ligand 2-(*N*-methylformimidoyl)pyridine was prepared according to the method for *N*-benzylidene-methylamine.¹¹ Ru(imin)₂(CN)₂ was prepared by the same method for Ru(L)₂(CN)₂ (L = bpy, phen) except that Ar gas was bubbled through the reaction mixture to prevent the oxidation of the ligand imin by O₂. The product was purified by column chromatography with methanol and recrystallized from acetone/hexane.¹²

For Ru(imin)₂(CN)₂, three diastereoisomers exist in contrast with L = bpy or phen analogues because of the asymmetry of the ligand L = imin. In Figure 1, the possible conformers are shown schematically:

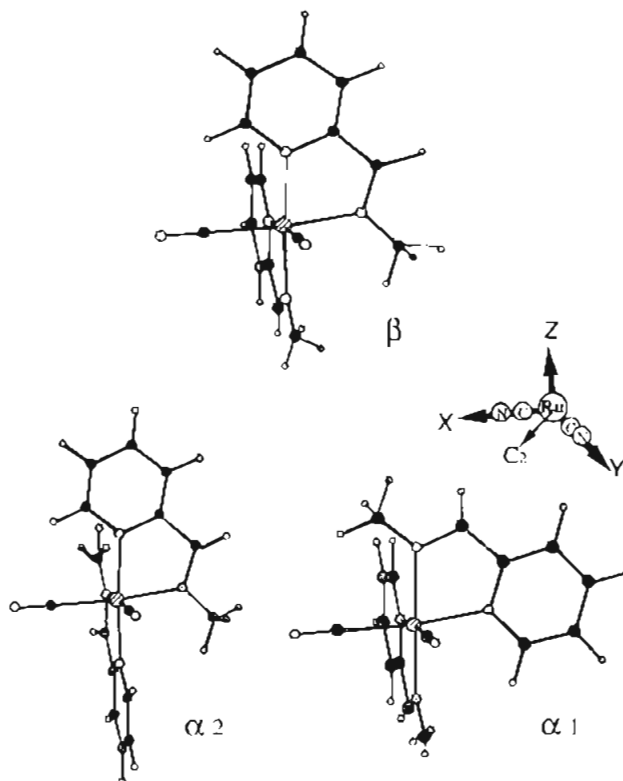


Figure 1. Schematic representations of the three possible diastereoisomers of Ru(imin)₂(CN)₂. The *xyz*-axis shown here is the one used for DV-X α MO calculations.

two of which are in C₂ symmetry, and the rest is in C₁ symmetry. These three isomers are referred to as α_1 ("ctc"), α_2 ("cct"), and β ("ccc") considering the conformation of the pair of CN and the coordinated nitrogen atoms of the imine and the pyridine unit following Krejčík et al.^{13a} and Goswami et al.^{13b} (Figure 1).

Four nonequivalent protons arise for each proton in the ligand L = imin from the mixture of these three diastereoisomers, two of which are from the nonequivalent two ligands of β conformer, one of which is from the equivalent two ligands of α_1 , and the rest of which is also from the equivalent two ligands of α_2 . By using the relative intensity of four singlet peaks of imine proton¹⁴ (C-CH=N-CH₃), the ratio of each diastereoisomer is roughly estimated as α_1 : α_2 : β = 6:1:4. α_1 and α_2 could be distinguished by the shift of the resonance position of the

- (5) (a) Cooper, J. B.; Vess, T. M.; Kalsbeck, W. A.; Wertz, D. W. *Inorg. Chem.* **1991**, *30*, 2286. (b) Cooper, J. B.; Wertz, D. W. *Inorg. Chem.* **1989**, *28*, 3108.
- (6) Winkler, J. R.; Sutin, N. *Inorg. Chem.* **1987**, *26*, 220.
- (7) Lippert, E.; Nägele, W.; Blankenstein, I. S.; Staiger, U.; Voss, W. Z. *Anal. Chem.* **1959**, *170*, 1.
- (8) Maruyama, M.; Sonoyama, N.; Kaizu, Y. *J. Phys. Chem.* **1994**, *98*, 5332.
- (9) *Organic Solvents*, 3rd ed.; Techniques of Chemistry; Wiley-Interscience: New York, 1979.
- (10) Demas, J. N.; Turner, T. F.; Crosby, G. A. *Inorg. Chem.* **1969**, *8*, 674.
- (11) (a) *Organic Synthesis*; John Wiley & Sons, Inc.: New York, 1965; Collective Vol. 3, p 258. (b) To a cooled solution of 2-pyridinecarboxaldehyde in benzene was added a 1.5 molar quantity of the methylamine solution of benzene. After 1 h of standing, the solvent was caused to reflux with a Dean-Stark water separator until no more water separated. After removal of the solvent, the product was distilled at 78–79 °C/18 mmHg.
- (12) Anal. Found: C, 44.54; H, 3.38; N, 19.58. Calcd for Ru(C₇N₂H₈)₂(CN)₂·2H₂O: C, 44.74; H, 4.66; N, 19.58.

- (13) (a) Krejčík, M.; Zalis, S.; Klima, J.; Sykora, D.; Matheis, W.; Klein, A.; Kaim, W. *Inorg. Chem.* **1993**, *32*, 3362. (b) Goswami, S.; Chakravarty, A. R.; Chakravorty, A. *Inorg. Chem.* **1983**, *22*, 602.
- (14) The chemical shifts (δ) of the imine (δ_1 , C-CH=N-CH₃) and methyl (δ_2 , C-CH=N-CH₃) protons are as follows (values in the brackets show the intensity of imine protons in arbitrary units): {compound, δ_1 [intensity], δ_2 } = { β , (8.65 ppm [2] and 8.81 ppm [2]), (3.40 ppm and 4.30 ppm)}, { α_1 , 8.84 ppm [6], 4.30}, { α_2 , 8.69 ppm [1], 3.19 ppm}. These assignments were based on ¹H-¹H COSY spectra.
- (15) (a) For example, Belser and Zelewsky^{15b} reported that the methyl proton of the ligand imin of Ru(bpy)₂(imin)²⁺, which was located over the pyridyl ring of bpy, was up-shifted by 0.15 ppm from the position of the free ligand. (b) Belser, P.; von Zelewsky, A. *Helv. Chim. Acta* **1980**, *63*, 1675.
- (16) (a) Streitwieser, A., Jr.; Heathcock, C. H. *Introduction to Organic Chemistry*, 3rd ed.; Macmillan Publishing Co.: New York, 1990; p 328. (b) To make sure that the proton over CN shows a downfield shift, we measured the ¹H-NMR spectra for some ruthenium(II) complexes which contain the CN ligand. For K₂Ru(bpy)(CN)₄, the 6, 6' protons of bpy, both of which are located over CN, show a downfield shift by 0.74 ppm (9.42 ppm in complex, 8.68 ppm in free ligand, in DMSO). For Ru(bpy)₂(CN)₂, one of the 6, 6' protons of bpy is located over CN and the other is over the pyridyl ring of the other bpy. The one which is located over CN shows a downfield shift by 1.00 ppm (9.68 ppm in the complex, 8.68 ppm in the free ligand, in CD₃OD). Such extent of the downfield shift is nearly identical with that (0.73 ppm) of the methyl proton of Ru(imin)₂(CN)₂ (α_1).

methyl proton ($C-CH=N-CH_3$) from the position of a free ligand (3.57 ppm); the methyl proton of α_2 is located above the pyridyl ring of the other ligand $L = \text{imin}$ and is upshifted by the ring current which induces the magnetic field opposite the applied field over the ring.¹⁵ On the other hand, the methyl proton of α_1 is located over the CN ligand and is downshifted by the circulating π -electrons of the triple bond around the symmetry axis which induces the magnetic field that adds to the applied field over (perpendicular to) the bond.¹⁶ The chromatographic separation of these diastereoisomers using a HPLC system has not been successful, which is attributed to the high polarity of these complexes which contain CN ligands.

DV-X α Computational Details. The DV-X α molecular orbital calculations¹⁷ were performed on a NEWS workstation (NWS-3460, Sony Co. Ltd.). Molecular geometry of all of the $Ru(L)_2(CN)_2$ complexes was assumed to C_2 symmetry: the metal atom was placed at the coordinate origin, two cyanides were on the x and y axes, and two polypyridine ligands L were in the $x-z$ and $y-z$ planes, respectively (see the xyz -axis in Figure 1). The bond lengths and angles of the Ru-bpy and Ru-phen parts were based on the crystallographic data of *cis*- $Ru(bpy)_2(CH_3CN)_2$ ¹⁸ and $Ru(DIP)_3$ ²⁺¹⁹ (DIP = 4,7-diphenyl-1,10-phenanthroline), respectively. The bond lengths of the Ru-CN part were estimated to be 2.019 Å (Ru-C) and 1.131 Å (C-N) from the crystallographic data of $Ru(DMPE)_2(CN)_2$ ²⁰ (DMPE = (dimethylphosphino)ethane). The C-H distance of the bpy ring was assumed to 1.08 Å on the basis of the value of pyridine.²¹ The calculation of $Ru(\text{imin})_2(CN)_2$ was carried out for the α_1 form which was the major product in the synthesis. The C-N framework of the ligand imin ($C=N=C-NC_5$) was assumed to be the same as the corresponding unit of bpy.²² The detailed bond lengths and angles of $L = \text{imin}$ used for calculations are summarized in supplementary Table 1, together with those of $L = \text{bpy}$ and phen.

Sample points were taken up to 50 000 points. Self-consistency within 0.001 e was obtained for orbital populations. The starting electronic configurations for the Ru, C, N, and H atoms were $(1s)^2(2s)^2(2p)^6(3s)^2(3p)^6(3d)^{10}(4s)^2(4p)^6(4d)^8(5s)^0(5p)^0$, $(1s)^2(2s)^2(2p)^2$, $(1s)^2(2s)^2(2p)^3$, and $(1s)^1$, respectively.

Results and Discussion

Spectroscopic Character of $Ru(\text{imin})_2(CN)_2$. The absorption and the corrected emission spectra of $Ru(\text{imin})_2(CN)_2$ in acetonitrile solutions are shown in Figure 2, together with those of $Ru(\text{bpy})_2(CN)_2$. The absorption bands in the visible region are assigned to the ¹MLCT transition. The energy of the lowest MLCT absorption maximum ($E_{\text{abs}}^{\text{max}}$) of $Ru(\text{imin})_2(CN)_2$ is considerably coincident with that of $Ru(\text{bpy})_2(CN)_2$ at around $20 \times 10^3 \text{ cm}^{-1}$. The values of $E_{\text{abs}}^{\text{max}}$ for $Ru(L)_2(CN)_2$ ($L = \text{bpy}$, imin, and phen) in various solvents are collected in Table 1. The $E_{\text{abs}}^{\text{max}}$ values in each solvent are nearly identical for three complexes studied in this work. This is consistent with the electrochemical data. As pointed out by Barigelletti et al.,²³ the gap between the oxidation potential (which corresponds to the energy needed to remove one electron from the metal ion) and the reduction potential (which corresponds to the energy needed to reduce the ligand) correlates with the MLCT transition

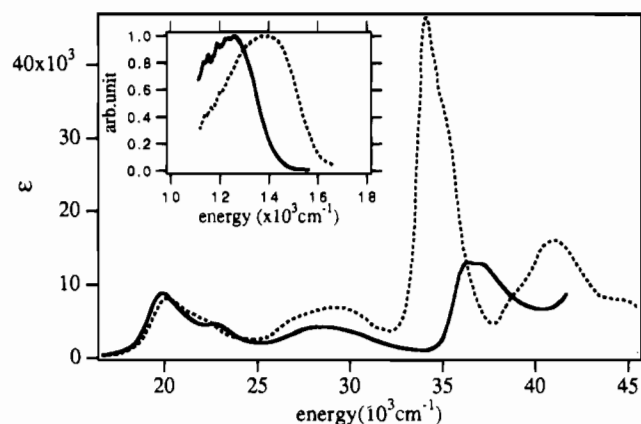


Figure 2. Absorption and emission spectra of $Ru(\text{imin})_2(CN)_2$ (bold line) and $Ru(\text{bpy})_2(CN)_2$ (dotted line) in acetonitrile solutions.

energy since the metal ion and the ligand are oxidized and reduced in the transition, respectively. The coincidence of the absorption maxima for $Ru(L)_2(CN)_2$ studied here comes from the fact that the oxidation and reduction potentials of these complexes are nearly identical.²⁴

The absorption band in the UV region is assigned to a ligand $\pi-\pi^*$ transition. The absorption maximum of $Ru(\text{imin})_2(CN)_2$ ($36 \times 10^3 \text{ cm}^{-1}$) is blue-shifted compared with that of $Ru(\text{bpy})_2(CN)_2$ ($35 \times 10^3 \text{ cm}^{-1}$).

The emission from the ³MLCT state of $Ru(\text{imin})_2(CN)_2$ is red-shifted compared with that of $Ru(\text{bpy})_2(CN)_2$ as shown in Figure 2. The values of $E_{\text{em}}^{\text{max}}$ in various solvents are collected in Table 1. $E_{\text{em}}^{\text{max}}$ of $Ru(\text{imin})_2(CN)_2$ is very small compared with that of $Ru(\text{bpy})_2(CN)_2$ and $Ru(\text{phen})_2(CN)_2$ in all solvents studied in this work. It should be noted that $E_{\text{em}}^{\text{max}}$ of $Ru(\text{phen})_2(CN)_2$ is larger than that of $Ru(\text{bpy})_2(CN)_2$ by 500 cm^{-1} , which corresponds to the larger $E_{\text{abs}}^{\text{max}}$ of $Ru(\text{phen})_2(CN)_2$ than that of $Ru(\text{bpy})_2(CN)_2$ to the same extent. In consistent with the energy gap law which predicts that the nonradiative decay rate increases with the decrease of the energy of the emission maximum, the lifetimes of $Ru(L)_2(CN)_2$ in CH_3CN become shorter in the order of $L = \text{phen}$ (1200 ns), bpy (270 ns), and imin (40 ns).

Since the ¹MLCT absorption maxima are nearly coincident for the three complexes, it follows that the Stokes shift (ΔE_{ST}), which means the difference between $E_{\text{abs}}^{\text{max}}$ and $E_{\text{em}}^{\text{max}}$, of $Ru(\text{imin})_2(CN)_2$ is larger than that of $Ru(\text{bpy})_2(CN)_2$ and $Ru(\text{phen})_2(CN)_2$. The values of ΔE_{ST} of $Ru(L)_2(CN)_2$ in various solvents are also summarized in Table 1. In Figure 3, ΔE_{ST} is plotted against Gutmann's solvent acceptor number (AN),^{25,26} which represents the Lewis acidity of the solvents. The AN dependencies of $E_{\text{abs}}^{\text{max}}$ and $E_{\text{em}}^{\text{max}}$ are also inserted in the same figure. It is found out that (i) both $E_{\text{abs}}^{\text{max}}$ and $E_{\text{em}}^{\text{max}}$ of $Ru(\text{imin})_2(CN)_2$ correlate with AN and that (ii) the solvent dependence of $E_{\text{em}}^{\text{max}}$ is weak compared with that of $E_{\text{abs}}^{\text{max}}$. These results

(17) The program developed by Prof. H. Adachi was used for these calculations.

(18) Heeg, M. J.; Kroener, R.; Deutsch, E. *Acta Crystallogr.* **1985**, *C41*, 684.

(19) Goldstein, B. M.; Barton, J. K.; Berman, H. M. *Inorg. Chem.* **1986**, *25*, 842.

(20) Jones, W. D.; Kosar, W. P. *Organometallics* **1986**, *5*, 1823.

(21) Bak, B.; Hansen-Nygaard, L.; Rastrup-Andersen, J. *J. Mol. Spectrosc.* **1958**, *2*, 361.

(22) (a) This conventional model will underestimate the N-Me bond length of imine unit by around 0.13 Å judging from the ordinal N-C length.^{22b} The extension of the bond by 0.13 Å gave the same calculational results. (b) *International Tables for Crystallography*; Kluwer Academic Publishers: Dordrecht, The Netherlands 1992; Vol. C, p 697.

(23) Barigelletti, F.; Juris, A.; Balzani, V.; Belser, P.; von Zelewsky, A. *Inorg. Chem.* **1987**, *26*, 4115.

(24) (a) The oxidation potential ($E(A/A^+)$) and the first reduction potential ($E(A^-/A)$) vs 0.1 M $Ag/AgNO_3$ in CH_3CN and the lifetime (τ) of $Ru(L)_2(CN)_2$ in CH_3CN at 298 K are as follows: (L, $E(A/A^+)$, $E(A^-/A)$, τ) = (imin, +0.50 V, -2.00 V, 40 ns), (bpy, +0.47 V, -1.97 V, 270 ns), (phen, +0.49 V, -1.99 V, 1200 ns). (b) It should be noted that $E_{\text{abs}}^{\text{max}}$ of $Ru(\text{imin})_2(CN)_2$ in H_2O is lower than that of $Ru(\text{bpy})_2(CN)_2$ and $Ru(\text{phen})_2(CN)_2$ by more than 1000 cm^{-1} . Unfortunately, we lack definite information on the relationship between $E_{\text{abs}}^{\text{max}}$ and the electrochemical data in this solvent since we cannot obtain the redox potentials of $Ru(L)_2(CN)_2$ in H_2O due to the low solubility of these complexes.

(25) Gutmann, V. *The Donor-Acceptor Approach to Molecular Interactions*; Plenum: New York, 1978.

(26) Mayer, U. *Pure Appl. Chem.* **1979**, *51*, 1697.

Table 1. Spectroscopic Data of Ru(L)₂(CN)₂ and Solvent Parameters

solvent	AN ^a	F(D,n) ^b	E (10 ³ cm ⁻¹)								
			L = imin			L = bpy			L = phen		
			E _{abs} ^{max c}	E _{em} ^{max d}	ΔE _{ST} ^e	E _{abs} ^{max}	E _{em} ^{max}	ΔE _{ST}	E _{abs} ^{max}	E _{em} ^{max}	ΔE _{ST}
N,N-dimethylformamide	16.0	0.275	19.6	12.4	7.2	19.7	13.9	5.8	20.1	14.4	5.7
acetonitrile	19.3	0.306	19.9	12.6	7.3	20.2	14.0	6.2	20.5	14.6	5.9
dimethyl sulfoxide	19.3	0.264	19.8	12.6	7.2	20.0	14.2	5.8	20.2	14.4	5.8
dichloromethane	20.4	0.218	19.8	12.6	7.2	20.0	14.7	5.3	20.4	15.0	5.4
chloroform	23.1	0.149	19.8	12.9	6.9	20.0	14.9	5.1	20.4	15.4	5.0
2-propanol	33.5	0.279	20.9	12.8	8.1	21.0	15.0	6.0	21.3	15.5	5.8
ethanol	37.1	0.289	20.9	12.6	8.3	21.5	15.0	6.5	21.6	15.4	6.2
1-propanol	37.9 ^f	0.279	20.9	12.7	8.2	21.4	15.0	6.4	21.7	15.6	6.1
formamide	39.8	0.281	21.3	12.8	8.5	22.0	15.2	6.8	22.3	15.7	6.6
methanol	41.3	0.308	21.3	12.7	8.6	21.9	15.1	6.8	22.2	15.6	6.6
water	54.8	0.321	22.5	12.9	9.6	23.8	15.6	8.2	23.8	15.7	8.1

^a Gutmann's solvent acceptor number cited from refs 25 and 26. ^b Solvent dielectric parameter. The values of the static dielectric constant (*D*) and refractive index (*n*) are from: *Organic solvents*, 3rd ed.; Techniques of Chemistry; Wiley-Interscience: New York, 1979. ^c Energy of the absorption maxima of the lowest MLCT transition. ^d Energy of the emission maxima. ^e Stokes shift (which is the energy difference between *E*_{abs}^{max} and *E*_{em}^{max}). ^f Evaluated from the Figure 13 in ref 26.

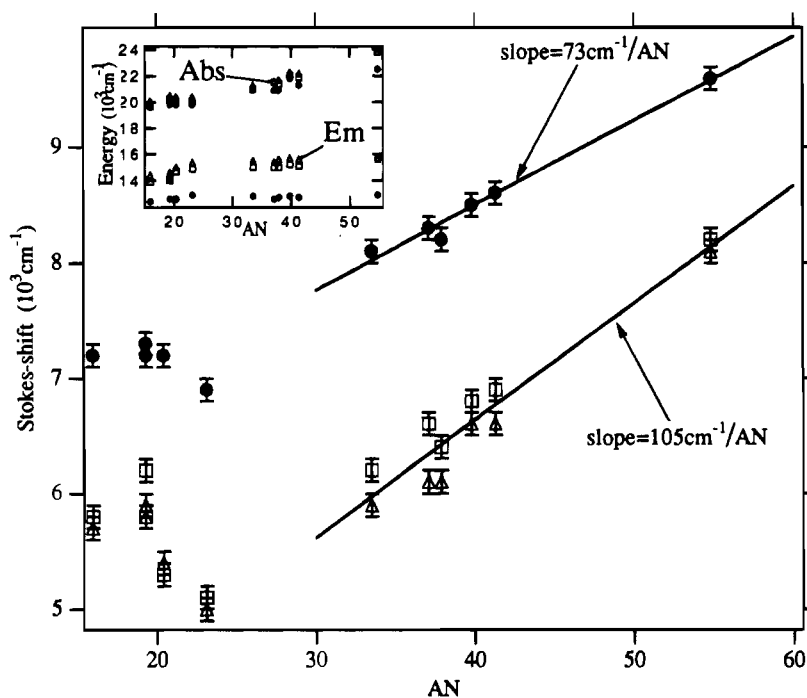


Figure 3. Plots of ΔE_{ST} of Ru(L)₂(CN)₂ vs AN (●, L = imin; □, L = bpy; △, L = phen). The inset is the plot of the absorption and the emission maxima of Ru(L)₂(CN)₂ vs AN.

are identical with the previous studies by other groups for Ru-(bpy)₂(CN)₂,²⁷ Ru(phen)₂(CN)₂,² and related complexes.^{1a,28}

For all the solvents studied in this work, the values of ΔE_{ST} of Ru(imin)₂(CN)₂ are larger than those of the Ru(bpy)₂(CN)₂ and Ru(phen)₂(CN)₂ complexes. The reason for the large ΔE_{ST} of Ru(imin)₂(CN)₂ is discussed later. The weak solvent dependence of ΔE_{ST} of Ru(imin)₂(CN)₂ compared with that of the L = bpy and phen analogues should be more emphasized here. For six protic solvents in Figure 3, the ΔE_{ST} values of Ru(imin)₂(CN)₂ show a good correlation with AN, similar to those of Ru(bpy)₂(CN)₂ and Ru(phen)₂(CN)₂. ΔE_{ST} increases with the increase of AN, which indicates that the solvent reorganization through the change of the acid–base interaction at the CN unit has a crucial effect on the degree of ΔE_{ST} in protic media. The slope of Ru(imin)₂(CN)₂ is smaller than that of Ru(bpy)₂(CN)₂ and Ru(phen)₂(CN)₂. The values of the slopes

obtained by the least-squares method are 73 cm⁻¹/AN and 105 cm⁻¹/AN for Ru(imin)₂(CN)₂ and for Ru(bpy)₂(CN)₂ and Ru(phen)₂(CN)₂, respectively. Since the points of Ru(bpy)₂(CN)₂ and Ru(phen)₂(CN)₂ lay nearby, the data for these complexes were analyzed together. The weak solvent dependence of ΔE_{ST} of Ru(imin)₂(CN)₂ indicates the smaller solvent reorganization at the CN unit for this complex in the excited state than for Ru(bpy)₂(CN)₂ and Ru(phen)₂(CN)₂.

There is not a complete enough correlation between ΔE_{ST} and AN to include all the data for protic and aprotic solvents. This is obviously caused from the weaker solvent dependence of *E*_{em}^{max} on AN compared with that of *E*_{abs}^{max} for Ru(L)₂(CN)₂,^{1a,2} which indicates that ΔE_{ST} (the difference between *E*_{abs}^{max} and *E*_{em}^{max}) shows positive deviations as the AN increases from aprotic to the protic solvents. Fung et al.²⁷ pointed out that the correlation was improved if the solvent dielectric parameter $1/n^2 - 1/D$ or $(1 - D)/(2D - 1)$, where *D* and *n* are the static dielectric constant and the refractive index of the solvent, respectively, was used in a dual-parameter fit along with AN.

(27) Fung, E. Y.; Chua, A. C. M.; Curtis, J. C. *Inorg. Chem.* **1988**, *27*, 1294.

(28) Mayer²⁶ reported the good correlation of the MLCT absorption maxima of Fe(L)₂(CN)₂ (L = 4,7-diphenyl-1,10-phenanthroline) with AN.

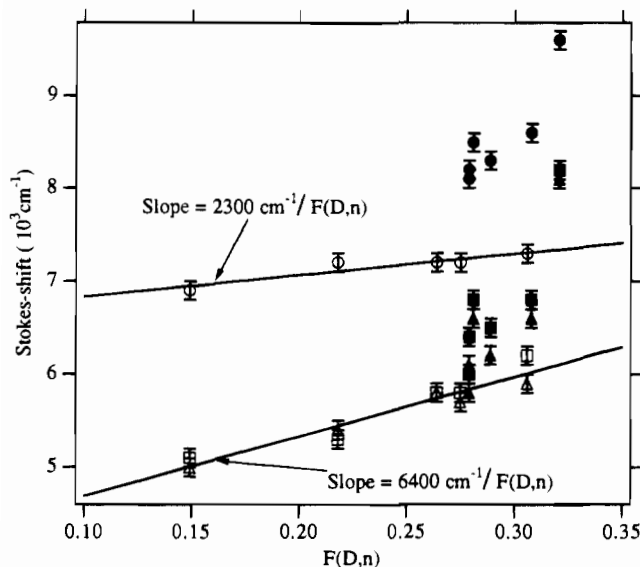


Figure 4. Plots of ΔE_{ST} of $\text{Ru}(\text{L})_2(\text{CN})_2$ vs $F(D,n)$ (○, L = imin; □, L = bpy; △, L = phen). The open and the filled symbols represent the data for the aprotic and for the protic solvents, respectively.

Since the correlation between ΔE_{ST} and AN in aprotic solvents is not clear, it is considered that the solvent reorganization process in aprotic solvents is different from that in protic solvents. In other words, in aprotic solvents, the degree of ΔE_{ST} is not governed so strongly by the specific base–acid interaction at CN as in protic solvents.

In Figure 4, the values of ΔE_{ST} are plotted against the solvent dielectric parameter $F(D,n)$ defined as

$$F(D,n) = \frac{D-1}{2D+1} - \frac{n^2}{2n^2+1} \quad (1)$$

The parameter $F(D,n)$ represents the dielectric polarity of the solvent around the polar solute. This reaction field parameter accounts for the Stokes shift of the fluorescence of aromatic compounds caused by the change of the dipole–dipole interactions between the solvent and solute in the excited state.^{29–31} We used $F(D,n)$ as the dielectric parameter of the solvent, not $1/n^2 - 1/D$ or $(1-D)/(2D-1)$,³² because the plot of the Stokes shift against $F(D,n)$ makes the estimation of the change of the dipole moment in the excited state from that of the ground state possible.^{29–31}

Rather good correlations are obtained for ΔE_{ST} against $F(D,n)$ for $\text{Ru}(\text{L})_2(\text{CN})_2$ in aprotic solvents. As the solvent polarity increases, ΔE_{ST} increases. This result indicates that the dielectric property of the solvent has a crucial effect on the degree of ΔE_{ST} of these complexes in the aprotic media. The dependence of ΔE_{ST} on $F(D,n)$ for $\text{Ru}(\text{imin})_2(\text{CN})_2$ is found to be smaller than that for $\text{Ru}(\text{bpy})_2(\text{CN})_2$ and $\text{Ru}(\text{phen})_2(\text{CN})_2$. The weak solvent dependence of $\text{Ru}(\text{imin})_2(\text{CN})_2$ in aprotic media indicates the small dielectric reorganization of the solvents in the excited state around this complex compared with that around L = bpy and phen analogues. The points for protic solvents for all $\text{Ru}(\text{L})_2(\text{CN})_2$ show positive deviations from the lines obtained for aprotic solvents, which indicates the additional

solvent reorganization through the acid–base interaction at the CN unit in these solvents.

Following Lippert–Mataga,^{29,30} the Stokes shift of the solute placed in the spherical cavity (whose radius is a) in the continuous dielectric media is represented as

$$\Delta E_{ST} = F(D,n) \times \frac{(\mu_{\text{ex}} - \mu_{\text{gr}})^2}{a^3} \quad (2)$$

where μ_{ex} and μ_{gr} are the dipole moment of the solute in the excited and the ground states, respectively. This equation shows that ΔE_{ST} is proportional to the square of the difference of the dipole moments between the ground and the excited states. The value of $|\mu_{\text{ex}} - \mu_{\text{gr}}|$ could be obtained from the slope of the plot of ΔE_{ST} against $F(D,n)$. Thus, the weak solvent dependence of ΔE_{ST} of $\text{Ru}(\text{imin})_2(\text{CN})_2$ implies the small change of the dipole moment in the excited state.

By using the values of the slopes shown in Figure 4 and the radius (a) of the spherical cavity (4.5 \AA),³³ $|\mu_{\text{ex}} - \mu_{\text{gr}}|$ was estimated to be 4.6 D for $\text{Ru}(\text{imin})_2(\text{CN})_2$ and 7.7 D for $\text{Ru}(\text{L})_2(\text{CN})_2$ (L = bpy and phen). Since the plots of $\text{Ru}(\text{bpy})_2(\text{CN})_2$ and $\text{Ru}(\text{phen})_2(\text{CN})_2$ lay nearby within the experimental error, the data were analyzed together for these complexes. It is found that the change of the dipole moment of $\text{Ru}(\text{imin})_2(\text{CN})_2$ in the excited state is smaller than that of L = bpy and phen derivatives.

Electronic Character of $\text{Ru}(\text{L})_2(\text{CN})_2$ in the Ground States. To know the electronic distribution of $\text{Ru}(\text{L})_2(\text{CN})_2$ in the ground and the MLCT excited states, the DV– $X\alpha$ molecular orbital calculations were carried out for $\text{Ru}(\text{L})_2(\text{CN})_2$ complexes where L = imin (α_1), bpy, and phen. In Figure 5, the energy diagrams of the frontier orbitals are shown for $\text{Ru}(\text{imin})_2(\text{CN})_2$ (α_1) and $\text{Ru}(\text{bpy})_2(\text{CN})_2$. The predominant character in percent was also shown for some of important orbitals. The detailed charge distributions on each atoms of frontier orbitals including $\text{Ru}(\text{phen})_2(\text{CN})_2$ were listed in supplementary Table 2.

For $\text{Ru}(\text{bpy})_2(\text{CN})_2$, the highest occupied orbitals 60a, 57b, and 59a are localized predominantly on the ruthenium 4 d_{π} orbitals described by d_{xy} , $(1/\sqrt{2})(d_{xz} + d_{yz})$, and $(1/\sqrt{2})(d_{zx} - d_{zy})$, respectively. These orbitals strongly interact with the π orbitals of CN and, to a lesser extent, interact with the π orbitals of the bpy. In these orbitals, the electronic localization on the ruthenium atom and the CN ion are 50–60% and $\approx 30\%$, respectively. The orbitals from 58a to 56a in the occupied orbitals are localized on the π and σ orbitals of CN, and below these, there exist the orbitals which are localized on the bpy π orbitals (53b and 55a). The lowest unoccupied orbitals 58b and 61a are localized on the bpy π^* orbitals. The characters of the frontier orbitals of $\text{Ru}(\text{imin})_2(\text{CN})_2$ and $\text{Ru}(\text{phen})_2(\text{CN})_2$ are the same as that of $\text{Ru}(\text{bpy})_2(\text{CN})_2$.

The degree of the electronic localization on the ruthenium atom for $\text{Ru}(\text{L})_2(\text{CN})_2$ (L = bpy, imin, phen) (50–60%) in the HOMO orbitals is very close to the value of $\approx 60\%$ obtained for $\text{Ru}(\text{diimine})_3^{2+}$ (diimine = $\text{H}-\text{N}=\text{C}-\text{C}=\text{N}-\text{H}$) by means of the $X\alpha$ calculations by Daul and Weber³⁴ and by Kobayashi et al.³⁵ The major difference between $\text{Ru}(\text{diimine})_3^{2+}$ and $\text{Ru}(\text{L})_2(\text{CN})_2$ is that the former has the large electronic population

(29) (a) Lippert, E. Z. *Elektrochem.* **1957**, *61*, 962. (b) Lippert, E. Z. *Phys. Chem.* **1956**, *6*, 125.

(30) (a) Mataga, N.; Kaifu, Y.; Koizumi, M. *Bull. Chem. Soc. Jpn.* **1955**, *28*, 690. (b) Mataga, N.; Kaifu, Y.; Koizumi, M. *Ibid.* **1956**, *29*, 465.

(31) Khundkar, L. R.; Stigman, A. E.; Perry, J. W. *J. Phys. Chem.* **1990**, *94*, 1224.

(32) It should be pointed out that the Stokes shift shows good correlations with these dielectric parameters as well.

(33) The distance from Ru to the outermost hydrogen of L = bpy is $\approx 7 \text{ \AA}$,¹⁸ and the distance from Ru to N atom of CN is $\approx 3 \text{ \AA}$.²⁰ Thus, the averaged radius of $\text{Ru}(\text{bpy})_2(\text{CN})_2$ could be roughly estimated as $\approx 5 \text{ \AA}$. The value $a = 4.5 \text{ \AA}$ was estimated by subtracting 0.5 \AA from the averaged radius taking into account the space between the ligands in which solvents will enter.

(34) Daul, C. A.; Weber, J. *Chem. Phys. Lett.* **1981**, *77*, 593.

(35) Kobayashi, H.; Kaizu, Y.; Matsuzawa, H.; Sekino, H.; Torii, Y. *Mol. Phys.* **1993**, *78*, 909.

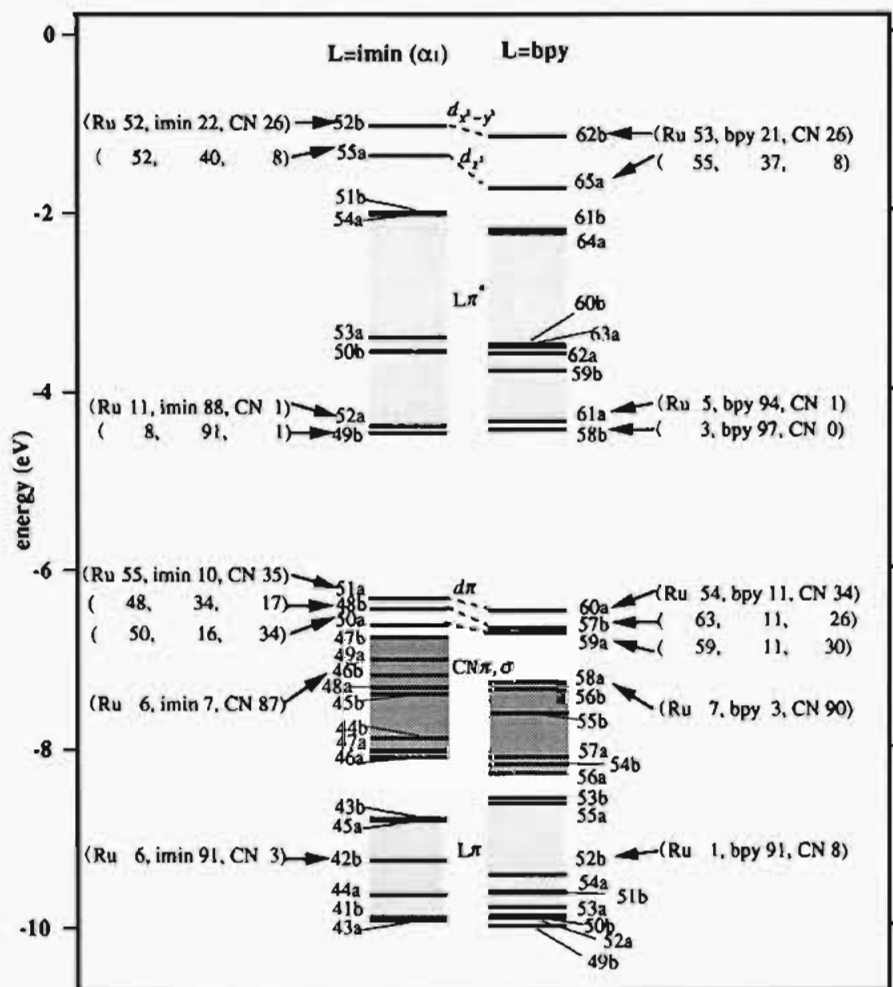


Figure 5. Frontier orbitals in the DV-X α calculations for Ru(L)₂(CN)₂. The predominant orbital characters (in percent) of selected orbitals are also shown.

on diimine ($\approx 30\%$) in these orbitals, while the latter has the small electronic population on L ($\approx 10\%$). Electronic mixing between the ruthenium d_{π} orbital and CN π orbital surpasses that between the ruthenium d_{π} orbital and L π orbital for Ru(L)₂(CN)₂.

The calculated absorption intensities are plotted against the excitation energy in Figure 6. The excitation energies are calculated by use of the transition-state method^{36,37} in which a half-electron is promoted from the ground state configuration to the excited state configuration. The absorption intensities are given in terms of the oscillator strength (f), which is evaluated from the excitation energies and transition dipole moments. The transition dipole moments are evaluated with the transition-state orbitals, which are a compromise between the initial and final state wave functions while keeping their orthogonality.

For Ru(imin)₂(CN)₂, the transition-state theory predicts the lowest MLCT bands (51a, 48b, and 50a \rightarrow 49b and 52a) at around $20 \times 10^3 \text{ cm}^{-1}$, the second MLCT band (51a \rightarrow 50b and 53a) at around $28 \times 10^3 \text{ cm}^{-1}$, and the π - π^* band (43b, 45a, 44a and 42b \rightarrow 49b and 52a) at around $(35 - 43) \times 10^3 \text{ cm}^{-1}$. It is found out that the calculations reproduce the absorption spectra of Ru(L)₂(CN)₂ (L = imin, bpy) well.

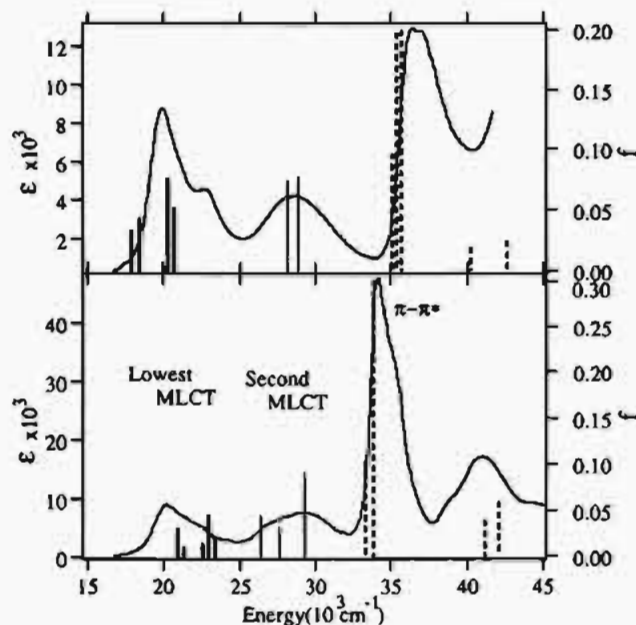


Figure 6. Energy levels of Ru(L)₂(CN)₂ (top, L = imin (α_1); bottom, L = bpy) evaluated by the transition state theory. Bold, plain, and broken lines represent the lowest MLCT, second MLCT, and π - π^* transitions, respectively. The absorption spectra in CH₃CN are also shown. Those in more nonpolar solvents such as CH₂Cl are not used for comparison because of the narrow window of the solvents. However, the absorption maxima in the visible region in those more nonpolar solvents coincide with those in CH₃CN within $100\text{--}200 \text{ cm}^{-1}$.

(36) (a) Slater, J. C.; Mann, J. B.; Wilson, T. M.; Wood, J. H. *Phys. Rev.* **1969**, *184*, 672. (b) Slater, J. C. *Advances in Quantum Chemistry*; Academic Press: New York, 1972; Vol. 6, p 1.

(37) Kobayashi, H.; Kaizu, Y.; Kimura, H.; Matsuzawa, H.; Adachi, H. *Mol. Phys.* **1988**, *64*, 1009.

Table 2. Net Charge (e) on Each Unit, Dipole Moment (μ), and the Change of the Net Charge (Δe) and the Dipole Moment ($\Delta\mu$) in the Excited States from Those in the Ground State for $\text{Ru}(\text{L})_2(\text{CN})_2$

	e (Ru)	L	CN	μ (debye) ^a	Δe (Ru)	L	CN) ^b	$\Delta\mu$ (debye)
L = bpy								
ground state	+0.726	+0.187	-0.550	-13.8				
MLCT excited states								
60a→58b	+0.807	+0.011	-0.414	-9.49	+0.081	-0.176	+0.136	+4.31
57b→58b	+0.817	+0.017	-0.425	-9.24	+0.091	-0.170	+0.125	+4.56
59a→58b	+0.818	+0.014	-0.423	-9.24	+0.092	-0.173	+0.127	+4.56
60a→61a	+0.805	+0.014	-0.416	-9.71	+0.079	-0.173	+0.134	+4.09
57b→61a	+0.815	+0.020	-0.427	-9.45	+0.089	-0.167	+0.123	+4.35
59a→61a	+0.816	+0.018	-0.426	-9.45	+0.090	-0.169	+0.124	+4.35
L = imin								
ground state	+0.739	+0.190	-0.559	-13.8				
MLCT excited states								
51a→49b	+0.814	+0.042	-0.449	-10.1	+0.075	-0.148	+0.110	+3.70
48b→49b	+0.793	+0.110	-0.506	-10.4	+0.054	-0.080	+0.053	+3.40
50a→49b	+0.807	+0.060	-0.463	-10.2	+0.068	-0.130	+0.096	+3.60
51a→52a	+0.811	+0.046	-0.451	-10.3	+0.072	-0.144	+0.108	+3.50
48b→52a	+0.789	+0.114	-0.508	-10.6	+0.050	-0.076	+0.051	+3.20
50a→52a	+0.804	+0.062	-0.464	-10.3	+0.065	-0.128	+0.095	+3.50

^a μ is directed along the C_2 axis of the molecule (see the inset of Figure 7). ^b The plus and the minus signs represent the decrease and increase of the electronic population in the excited state, respectively.

Electronic Flow of $\text{Ru}(\text{L})_2(\text{CN})_2$ in the MLCT Excited States. In Table 2, the net charges on three units (i.e., Ru, L, and CN) of $\text{Ru}(\text{L})_2(\text{CN})_2$ in the ground and the lowest MLCT excited states are shown, together with the change of the net charge of the excited states from the ground state. The data for $\text{Ru}(\text{phen})_2(\text{CN})_2$ are also collected in supplemental Table 3. The electronic distribution of the lowest MLCT configurations are obtained by promoting one electron from three HOMOs (whose main character is the ruthenium d_π orbital) to the low-lying two LUMOs (whose main character is L π^* orbital).

It is found that the positive charge on the Ru atom increases, the negative charge on the CN decreases, and the positive charge on L decreases in the MLCT transitions, which mean the decrease of the electronic population on Ru and CN and the increase of it on L. In the ground state of $\text{Ru}(\text{bpy})_2(\text{CN})_2$, the net charges on Ru, L, and CN are +0.726 e , +0.187 e , and -0.550 e , respectively. In the excited state (60a→58b), the positive charge on Ru increases by 0.081 e , the negative charge on CN decreases by 0.136 e , and the positive charge on L decreases by 0.176 e . Due to the large electronic migration from L to Ru and CN in the excited states, the electronic population on L does not increase so much even though one electron is promoted from HOMO to LUMO orbitals. It should be noted that the decrease of the electronic population on CN is comparable or slightly larger than that on Ru. The decrease of the electronic population on CN leads to the increase of the acidity of this unit in the excited state. Thus, our calculational results are consistent with the experiment of Peterson and Demas,³ who found that the deprotonation of the protonated $\text{Ru}(\text{bpy})_2(\text{CN})_2$ and $\text{Ru}(\text{phen})_2(\text{CN})_2$ occurred following the light excitation and also the weak AN dependence of the emission of $\text{Ru}(\text{L})_2(\text{CN})_2$ in comparison with that of the absorption.^{2,27}

The decrease of the electronic population on CN of $\text{Ru}(\text{imin})_2(\text{CN})_2$ is smaller than that of $\text{Ru}(\text{bpy})_2(\text{CN})_2$ and $\text{Ru}(\text{phen})_2(\text{CN})_2$. The negative charges on CN of $\text{Ru}(\text{bpy})_2(\text{CN})_2$ and $\text{Ru}(\text{phen})_2(\text{CN})_2$ decrease by 0.123–0.136 e and 0.110–0.136

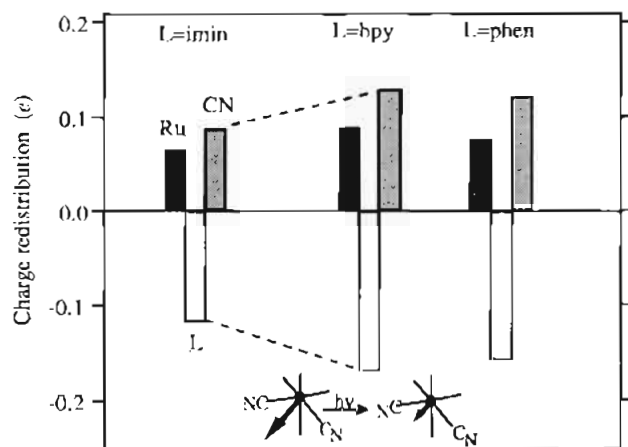


Figure 7. Schematic representation of the change of the net charge on each unit of $\text{Ru}(\text{L})_2(\text{CN})_2$. The plus and minus signs represent the decrease and the increase of the charge, respectively. The inset represents the change of the dipole moment of $\text{Ru}(\text{L})_2(\text{CN})_2$ in the MLCT excited states.

e in the six lowest MLCT transitions, respectively, while that of $\text{Ru}(\text{imin})_2(\text{CN})_2$ decreases only by 0.053–0.110 e . The decreases of the negative charge on CN in the six lowest MLCT transitions are 0.128 e , 0.121 e , and 0.068 e in average for $\text{Ru}(\text{bpy})_2(\text{CN})_2$, $\text{Ru}(\text{phen})_2(\text{CN})_2$, and $\text{Ru}(\text{imin})_2(\text{CN})_2$, respectively. In Figure 7, the averaged changes of the net charge on the CN, Ru atom, and L in the six transitions are plotted schematically for each $\text{Ru}(\text{L})_2(\text{CN})_2$. The increase of the positive charge on Ru of $\text{Ru}(\text{imin})_2(\text{CN})_2$ (0.064 e) is not so different from that of $\text{Ru}(\text{bpy})_2(\text{CN})_2$ (0.087 e) and $\text{Ru}(\text{phen})_2(\text{CN})_2$ (0.076 e). The decrease of the positive charge on L of $\text{Ru}(\text{imin})_2(\text{CN})_2$ (0.118 e) is smaller than that of $\text{Ru}(\text{bpy})_2(\text{CN})_2$ (0.171 e) and $\text{Ru}(\text{phen})_2(\text{CN})_2$ (0.159 e). Such a small electronic redistribution of $\text{Ru}(\text{imin})_2(\text{CN})_2$ in the excited state, that is, the small decrease of the electronic population on CN and the small increase of it on L, is considered to come from the smaller π electron system

of the ligand L = imin, which will hold less electrons in the MLCT excited states compared with that of L = bpy and phen. The brief calculations of the electronic flow in the excited states for the α_2 conformer of Ru(imin)₂(CN)₂ gave qualitatively the same results as the α_1 .

The smaller decrease of the electronic population on CN of Ru(imin)₂(CN)₂ means the smaller increase of the Lewis acidity of CN of this complex compared with that of Ru(bpy)₂(CN)₂ and Ru(phen)₂(CN)₂ in the MLCT excited states. This indicates that the solvent reorganization caused from the change of the acid-base interaction around CN in the excited state is smaller for Ru(imin)₂(CN)₂. Thus, the small decrease of the electronic population on CN of Ru(imin)₂(CN)₂ is considered to be the reason for the weak AN dependence of ΔE_{ST} of this complex in protic media.

Dipole Moment of Ru(L)₂(CN)₂ in the Ground and the MLCT Excited States. Molecular dipole moment μ of Ru(L)₂(CN)₂ could be estimated by

$$\mu = \sum_p q_p r_p \quad (3)$$

where q_p and r_p are the net charge and the point vector of the atom p, respectively. In Table 2, the dipole moments of Ru(L)₂(CN)₂, where L = bpy and imin (α_1) in the ground and the lowest MLCT excited states, are collected, together with the changes of the dipole moments in the excited states from that in the ground state.

The dipole moments of Ru(L)₂(CN)₂ in the ground state are directed along the C₂ axis toward the CN side, and their values are 13.8 D for both L = bpy and imin (α_1) and 13.9 D (supplemental Table 3) for L = phen. The dipole moment in the ground state comes from the negatively charged CN and the positively charged L.

In the excited state, the magnitude of the dipole moment decreases keeping their direction along the C₂ axis (see the inset of Figure 7). In the excited state (60a–58b) of Ru(bpy)₂(CN)₂ and (51a–49b) of Ru(imin)₂(CN)₂, the dipole moments decrease to 9.49 and 10.1 D, respectively. The decrease of the dipole moment in the excited state comes from the decrease of the electronic population on CN and the increase of it on L. The decrease of the dipole moment of Ru(L)₂(CN)₂ is, however, not the same. The decrease of the dipole moment of Ru(imin)₂(CN)₂ is smaller than that of others; in the six MLCT excited states, the dipole moments of Ru(bpy)₂(CN)₂ and Ru(phen)₂(CN)₂ decrease by 4.09–4.56 D and 4.34–4.77 D, respectively, while that of Ru(imin)₂(CN)₂ decreases only by 3.20–3.70 D.

The degree of the decrease of the dipole moment ($\Delta\mu$) of Ru(L)₂(CN)₂ in the excited states is affected by two factors, that is, (1) the size and the direction of the spread of the π -conjugation of L and (2) the total electronic density on L in the excited state. $\Delta\mu$ becomes large when the π -conjugation of L spreads far toward the opposite side of CN (toward the -x and -y directions, not $\pm z$ direction³⁸ in Figure 1) and the promoted electron could be spread far from the central ruthenium, since $\Delta\mu$ is proportional to the point vector (r_p) of atoms. $\Delta\mu$ also becomes large when the amount of the electron which is held in L in the excited state is large, since $\Delta\mu$ is proportional to the change of the net charge (q_p) on each atom.

The obtained small decrease of the dipole moment for Ru(imin)₂(CN)₂ (α_1) is considered to come mainly from (2), not

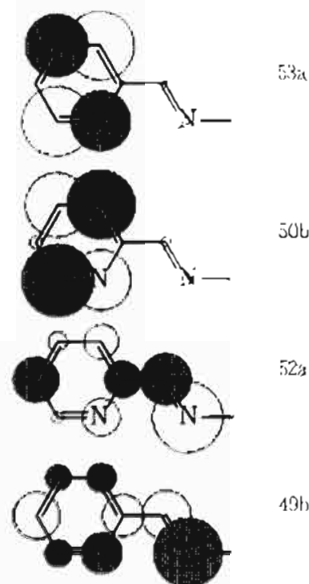


Figure 8. π^* contributions of L to the lowest vacant orbitals for Ru(imin)₂(CN)₂. Each circle is drawn in such a way that its radius represents the coefficient of the π^* orbital of each atom. The open and the shaded circles represent the plus and the minus signs of the coefficient, respectively.

from (1), since the spread of the π conjugation of L toward the -x and -y directions of Ru(imin)₂(CN)₂ (α_1) is not so different from that of Ru(bpy)₂(CN)₂ and Ru(phen)₂(CN)₂; the pyridyl ring of Ru(imin)₂(CN)₂ (α_1) is located in that direction (Figure 1) such as Ru(bpy)₂(CN)₂ and Ru(phen)₂(CN)₂.

The importance of the direction of the spread of the π -conjugation of L for $\Delta\mu$ will be made clearer by considering $\Delta\mu$ of the diastereoisomer α_2 of Ru(imin)₂(CN)₂. In this complex, there exists the small -CH=N-Me π -conjugation in the -x and -y directions (Figure 1). Thus, $\Delta\mu$ of α_2 should become smaller than that of α_1 . The brief calculation of Ru(imin)₂(CN)₂ (α_2) shows that $\Delta\mu$ is smaller (1.75–2.75 D) than that of α_1 (3.20–3.70 D) although the total electronic population on L in the excited state is the same for these complexes.

The calculational result that the decrease of the dipole moment of Ru(imin)₂(CN)₂ in the excited states is smaller than that of Ru(bpy)₂(CN)₂ and Ru(phen)₂(CN)₂ is in qualitative agreement with the result obtained from the solvent dependence of the ΔE_{ST} on $F(D, n)$ in aprotic solvents. The weak solvent dependence of ΔE_{ST} of Ru(imin)₂(CN)₂ compared with that of Ru(bpy)₂(CN)₂ and Ru(phen)₂(CN)₂ led to the small $\Delta\mu$ for the former (4.6 D for Ru(imin)₂(CN)₂ and 7.7 D for Ru(bpy)₂(CN)₂ and Ru(phen)₂(CN)₂). Thus, it is concluded that the small dielectric reorganization of the solvents due to the small decrease of the dipole moment of Ru(imin)₂(CN)₂ in the excited states is the reason for the weak solvent dependence of ΔE_{ST} of this complex in aprotic media.

Reason for the Large Stokes Shift of Ru(imin)₂(CN)₂. In the following, the reason for the large ΔE_{ST} of Ru(imin)₂(CN)₂ compared with that of the L = bpy or phen analogues is discussed. As shown in Table 1, ΔE_{ST} of Ru(imin)₂(CN)₂ is larger than that of others in all the solvents by 1000–2000 cm⁻¹. In general, the large Stokes shift is explained by two reasons, that is, the large (1) outer-sphere (solvent) and/or (2) inner-sphere reorganization in the excited state. As mentioned above, however, the solvent reorganization around Ru(imin)₂(CN)₂ is smaller than that around other Ru(L)₂(CN)₂ because of the smaller decrease of the electronic charge on CN and also the smaller change of the dipole moment in the excited state. Thus, the large inner-sphere reorganization in the MLCT excited states

(38) The spread of the π -conjugation of L toward the z or -z axis has no effect on the dipole moment ($\mu = \sum_p q_p \times r_p$) since the z-component of the products of q_p and r_p for each atom in one L is canceled by that of the equivalent atom of the other L because of the C₂ symmetry of Ru(L)₂(CN)₂.

is considered to be the main factor for the large ΔE_{ST} of Ru(imin)₂(CN)₂.

For Ru(imin)₂(CN)₂, relatively localized electronic character on the less rigid C=N bond of the methylimine in the lowest MLCT excited states is considered to cause the large inner-sphere distortion in the excited state. In the 53a and 50b orbitals, which lie at about 1 eV higher from the lowest vacant orbitals 52a and 49b, the electron is localized on the pyridyl ring (the ratios of the localization to the whole L of these orbitals are 100% and 99%, respectively), while, in the lowest vacant orbitals 52a and 49b, the electron is relatively localized on the methylimine C=N bond. The ratios of the localization on C=N to the whole L of these orbitals are 53% and 49% for 52a and 49b, respectively. In Figure 8, the charge distributions on L in these vacant orbitals are shown schematically. The electronic localization on the less rigid C=N bond in the antibonding phase in the lowest vacant orbitals (52a and 49b) from which the emission will occur is considered to result in the large bond distortion in the excited state.

Such a bond distortion in the MLCT excited state was also reported for the azo N=N bond by Wolfgang et al.³⁹ for the ruthenium(II) complexes which contain the ligand L = 2-(phenylazo)pyridine. A series of Ru^{II}(L)₂(L') and Ru^{II}(L)₂(L'')₂ complexes where L' and L'' represent the ligands such as acac (=2,4-pentanedionato) and NO₂ show the highly red-shifted emission due to the large inner-sphere reorganization. On the other hand, such a large inner-sphere reorganization is not likely to occur in the ligands bpy and phen which consist of rigid aromatic rings. It is concluded that the inner-sphere reorganization in the ligand L = imin in the lowest MLCT excited states is the main reason for the large ΔE_{ST} of Ru(imin)₂(CN)₂.

Summary

The weak solvent dependence of ΔE_{ST} for Ru(imin)₂(CN)₂ in protic and in aprotic solvents has been discussed in terms of the small decrease of the electronic population on CN and the small change of the dipole moment in the MLCT excited states, respectively. The small redistribution of the electron in the photo-excitation process from the ground to the MLCT excited states for Ru(imin)₂(CN)₂ is considered to come from the small size of the ligand L = imin which holds less electrons in the excited state compared with that of the ligand L = bpy and phen. Similar lack of solvent dependence of the MLCT states was also reported by Johnson and Trogler⁴⁰ for iron-DAB complexes (DAB = 1,4-diazabutadiene) which have smaller α,α' -diimine π -electron systems than imin or bpy. The large ΔE_{ST} of Ru(imin)₂(CN)₂ is considered to be caused from the large inner-sphere reorganization of the C=N bond of the methylimine on which the electron is relatively localized in the lowest MLCT states.

Acknowledgment. We thank Dr. H. Kimura for the instruction in the DV-X α calculations and Dr. M. Asano-Someda for the measurement of the emission spectra by the single-photon-counting method.

Supplementary Material Available: A table of bond lengths and angles of Ru(L)₂(CN)₂ (L = bpy, imin (α_1), and phen) used for the DV-X α calculations, a table listing the charge distribution of Ru(L)₂(CN)₂ (L = bpy, imin (α_1), and phen) in the ground state and a figure showing the numbering of atoms, and a table listing the net charge on each unit and the dipole moment of Ru(phen)₂(CN)₂ in the ground and the MLCT excited states (8 pages). Ordering information is given on any current masthead page.

IC9406188

(39) Wolfgang, S.; Streckas, T. C.; Gafney, H. D.; Krause, R. A.; Krause, K. *Inorg. Chem.* **1984**, *23*, 2650.

(40) Johnson, C. E.; Trogler, W. C. *J. Am. Chem. Soc.* **1981**, *103*, 6352.